# Response to referee O.P. Savchuk

We again thank the referee for his valuable comments on the manuscript. In addition to our previous response we will here provide som further comments on the changes that have been made in accordance with the referee feedback.

1.1 We have removed implications of causality where possible. We do however retain the word "causes" in the title with reference to our earlier reply.

1.2 We have removed the observational part. We have instead chosen to present the time-series and the wavelet spectrum of the simulated phytoplankton biomass together with the month of maximum chlorophyll maxima in Sect. 3.1. We have tried to make it clear that we are using only simulated variables.

1.3 We have changed to "phytoplankton biomass" as well as added a comment on the constant C:Chl ratio in Sect. 2.2.

1.4 We have removed discussions around the seasonal time-scale where possible. We have kept comments on the seasonal scale for the clear regime shift shown in current Fig. 10.

1.5 Again, we have removed the observational parts from the manuscript.

1.6 We have tried to improve the structuring and motivation for the manuscript mainly in the introduction and throughout Sect. 3. Much of the justification certainly boils down to the use of a relatively new tool. However, as a similar analysis has not previously been done for simulated biogeochemical variables we feel that an illustration of its uses is valuable.

2.1 We have changed the title to: Causes of simulated long-term changes in phytoplankton biomass in the Baltic Proper: A wavelet analysis.

2.2 We have removed "internal loads" where possible.

2.3 As stated in 1.6, we have tried to rework the introduction and section 3 in accordance with the referee comments.

2.4 This has been corrected.

2.4.1 We have removed unimportant equations from section 2. We have also removed the faulty comment on phosphate and salinity.

2.4.2 We have clarified that it is only around the study area.

2.5.1 The comparison with observations have been removed

2.5.2 We have removed discussion on the seasonal scale for the riverine input. We have further rewritten the section so that it is clear that we do not imply causality. We have also removed previous Figs 6 and 7.
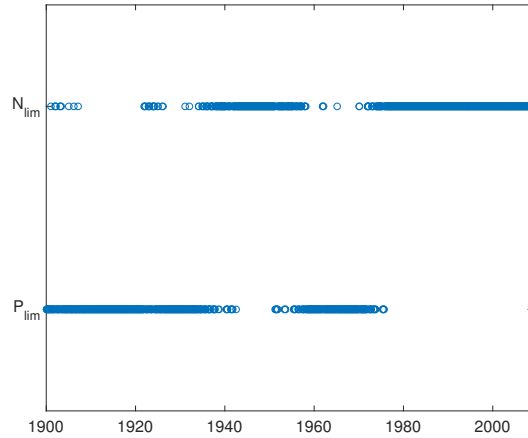
Figure 1: Nitrogen or phosphate limitation as calculated with N/P ratios.

2.5.3 We have added a comment on that Nlim can become larger than one (but not NUTLIM). However, as NUTLIM is what directly affects the phytoplankton growth in the model we have kept this formulation. We have added a discussion on that N/P ratios gives a different result more inline with observations in Sect. 3.2 (see Fig. 1).

We have also added a note in the figure caption that simultaneous N and P limitation is not possible.

2.5.4 For some quantities this might be helpful but we prefer the mixed layer concept, as is much more straight forward when it comes to the physical quantities. The sharp pycnocline inhibits vertical transfer, and is therefore a more natural choice for studying variations in N and P concentrations.

2.5.5 We have tried to rework the section (now 3.2) so that the purpose of the section is more clear. We have kept the figure showing our model results for anoxic volume and deep water nutrients (now Fig. 5) since we believe it to be necessary for the discussion.

3. We have adressed the minor comments.

# Response to Referee #3

We again thank the referee for the valuable comments. Referee comments in italics.

We have shortened section 2.2 and removed unnecessary equations.

- *Already in the abstract combination of words mixed layer parameter concentrations appears as solid term. However I did not find in the text how it was defined. Is it mean value of horizontal mean parameter in horizontal mean mixed layer? or it is integrated characteristic?*

  We have clarified that the parameters are horizontally and depth *averaged* and not integrated.

- *Salinity in the Baltic Sea and in the Baltic Proper have strong lateral gradient. However, mixed layer depth (MLD) was defined as constant density difference. Could it be that with decrease of salinity MLD will increase? Could it be that seasonal variability in surface effects MLD and at the end all results ? The part with mixed layer definition should be extended and some how emphasized. Maybe it makes sense to include it as additional subsection.*

  Changes in salinity will effect the mixed layer depth due to its effect on density, but this is captured in the definition of mixed layer as long as the equation of state used to calulate the density difference depends on salinity. The definition also captures the seasonal changes in mixed layer depth when monthly mean profiles of salinity and temperature are used in the calculation. The mixed layer definition is also standard and frequently used both in models and on observational data.

- *The basin integrated approach was used here (line 61). Would be good to see in the text why this is acceptable (preferably in more than one sentence, line 6*

  We have added a comment in section 2.1.

- *While SCOBI model is 1D model (line 67), I would suggest to show results of wavelet analysis for idealized 1D cases. So it could be seen how certain changes are reflected in final results of wavelet analysis. For my opinion such sensitivity test could enhance conclusions. Otherwise, section 2.4 should be extended with some aspects of wavelet coherence.*

  We have improved section 2.4 to provide a better description of the wavelet transform and wavelet coherence.

- *Analysis focuses mainly on river loads and its changes. Other nutrient sources like atmospheric deposition, exchange with other Baltic Sea regions and there possible effect should be mention somehow*

  We have tried during the revision work to include the atmospheric deposistion. Sadly, we only had yearly averaged values of the deposition to work

with and that is not good enough for the wavelet analysis. The horizontal transports suffers from a similar problem. Here we have the velocity fields and concentration fields but not their products, and we thus do not really know the transports. In future work we plan to close these nutrient budgets using online calculations, but in this current effort we have settled to look at correlations with some of the most important forcings.

- *It could be considered to include wavelet analysis in to the title to my opinion application of this method is among the most interesting aspects of this manuscript*

  We have changed the title in accordance with the review comment.

- *Line 75: eq. 1. NFIX is nitrogen fixation term, in all phytoplankton groups it looks strange. Is it a misprint?*

  We found the equation to be unnecessary and have therefore removed it.

- *Line 78: SINKIphy / SINKOphy is it sinking of phytoplankton?*

  We have removed the equation.

- *Lines 177 - 181: Paragraph is confusing. It starts with sentence about open boundary, but last two sentences are probably about river loads. Please specify in more details: what these assumption were applied to*

  We have rewritten.

# Causes of simulated ~~, longterm~~ long-term changes in ~~chlorophyll concentrations~~ phytoplankton biomass in the Baltic ~~Sea~~Proper: A wavelet analysis

Jenny Hieronymus[1], Kari Eilola[1], Magnus Hieronymus[1], H. E. Markus Meier[2,1], and Sofia Saraiva[1]

[1]Research and Development Department, Swedish Meteorological and Hydrological Institute, Norrköping, Sweden
[2]Department of Physical Oceanography and Instrumentation, Leibniz Institute for Baltic Sea Research Warnemünde, Rostock, Germany.

*Correspondence to:* Jenny Hieronymus (jenny.hieronymus@gmail.com)

**Abstract.** The co-variation of key variables with ~~modelled phytoplankton concentrations~~ simulated phytoplankton biomass in the Baltic proper has been examined using wavelet analysis and results of a long-term simulation for 1850-2008 with a high-resolution, coupled physical-biogeochemical circulation model for the Baltic Sea. By focusing on ~~interannual~~ inter-annual variations it is possible to track effects acting on decadal time scales such as temperature increase due to climate change as well as changes in nutrient input. The results indicate the largest inter-annual coherence of phytoplankton biomass with the limiting nutrient.However, after 1950 the coherence is reduced due to high mixed layer nutrient concentrations diminishing the effect of smaller long-term variations. Furthermore, the inter-annual coherence of mixed layer nitrate with riverine input of nitrate is much larger than the coherence between mixed layer phosphate and phosphate loads. This indicates a greater relative importance of ~~internal loads i.e.~~ mixing of phosphate from deeper layers. In addition, shifts in nutrient patterns give rise to changes in phytoplankton nutrient limitation. The modelled pattern shifts from purely phosphate limited to a seasonally varying regime. The results further indicate some effect of inter-annual temperature increase on cyanobacteria and flagellates. Changes in mixed layer depth affect mainly diatoms due to a high sinking velocity while inter-annual coherence between irradiance and phytoplankton is not ~~observed.~~ found.

## 1 Introduction

The Baltic Sea is a semi-enclosed brackish water body separated from the North Sea and Kattegat through the Danish Straits. It stretches from about $54^o$ to $66^o$ N and the limited water exchange with the ocean in the south gives rise to a large meridional salinity gradient. The circulation is estuarine with a salty ~~deepwater~~ deep-water inflow from the ocean and a fresher surface outflow. The Baltic Sea comprises a number of sub-basins connected by sills further restricting the circulation.

The limited water exchange and the long residence time of water have consequences for the ~~functioning of the~~ biology and the biogeochemistry. The Baltic Sea is naturally prone to eutrophication and organic matter degradation keeps the deep water oxygen concentrations generally low in between deep water renewal events. In turn, this leads to complex nutrient cycling with different processes acting in oxygenized vs low oxygen environments.

The Baltic Sea has experienced ~~extensive~~ anthropogenic pressure over the last century. After 1950~~an~~, intensive use of agricultural fertilizer greatly enhanced the nutrient loads. ~~Due to great improvements in sewage treatment the loads decreased again after 1980 (Gustafsson et al., 2012) .~~

~~The intensification in nutrient loads~~ This led to an expansion of hypoxic bottoms (Carstensen et al., 2014)~~. This has had effects on~~, in turn affecting the cycling of nutrients through the system. Anoxic sediments have lower phosphorus retention capacity resulting in increased deep water phosphate concentrations. Thereby, the flux of phosphate to the surface intensifies even though the external loads have decreased after 1980 in response to improved sewage treatment. Furthermore, as the anoxic area increases, the ~~boundary between anoxic and oxic sediments~~ area of interface between oxic and anoxic zones where denitrification occurs also increases. This results in a loss of nitrogen. Vahtera et al. (2007) described these processes as generating a "vicious circle" where decreased DIN concentrations together with increased phosphate enhance the relative importance of nitrogen fixation by cyanobacteria.

The importance of this coupling between oxygen and nutrients have been further examined in models. Gustafsson et al. (2012) confirmed, using the model BALTSEM, that internal nutrient recycling has increased due to reduced phosphate retention capacity, implicating a self sustained eutrophication where enhanced internal loads outweigh external load reductions.

~~In addition to the biogeochemical shifts in the Baltic Sea environment during the 20th century, sea surface temperatures have increased (Siegel et al., 2006) . This has an effect on the growth rate of phytoplankton as well as the speed of other biological processes~~Satellite monitoring has made it possible to observe changes in several physical and ecological surface variables during the past three decades. Significant changes in seasonality have been observed, such as earlier start of phytoplankton growth season and timing of chlorophyll maxima (Kahru et al., 2016) .

~~From satellite data, Kahru et al. (2016) detected a prolonged productive season as well as a chlorophyll maxima shifted towards the maximum cyanobacteria concentration in July. The effect of temperature on the growth rate and stratification is likely to have positively affected the strength of cyanobacteria blooms as well as the length of the growth season.~~

~~Schimanke and Meier (2016) analyzed multidecadal variations in Baltic Sea salinity and the coherence with different physical drivers. They used the wavelet transform to identify periodicities and wavelet conherency to analyse the driving mechanisms~~Although the satellite record is already substantial and growing, interannual shifts and variations over the past century can not be investigated in this way. Furthermore, the satellite record is restricted to a few surface variables. Shifts in nutrient composition and deep water variables remain difficult to evaluate using observations. Even though the Baltic Sea has a dense observational record from ships, stations and satellites, the longest nutrient records comprise station data from the early 70s (HELCOM, 2012) . For multidecadal periods of gap free data the use of a model is required.

In this paper we construct a thorough analysis of the co-variation of phytoplankton ~~concentration~~ biomass with key variables that have been affected by anthropogenic change over the 20th century. Using the biogeochemical model SCOBI (Eilola et al., 2009; Almroth-Rosell et al., 2011) coupled to the 3d circulation model RCO we scrutinize the effect of nutrient loads, nutrient concentration, temperature, irradiance and mixed layer depth on the modelled phytoplankton community.

The ~~effect of anoxia on the nutrient limitation and on the primary production is complex. In addition to decreased phosphorus retention capacity and denitrification, nitrification ceases in anoxic environments ultimately resulting in increased ammonium~~

concentrations (Conley et al., 2009) . ~~To elucidate the effect on the primary production, we calculate the degree of nutrient limitation and its correlation with phytoplankton.~~ gap-free dataset provided by the model lets us decompose the variables in time-frequency space using the wavelet transform. Two variables may than be compared using wavelet coherence (eg. Torrence and Compo,

We have chosen to use a model run spanning 1850-2009. Thereby, we capture conditions relatively unaffected by anthropogenic forcing as well as current conditions of eutrophication and climate change. Furthermore, we limit our investigation to the Baltic Proper so as to capture relatively homogenous conditions with regards to the ~~functioning of the biology. Our main focus lies in inter-annual variations although some seasonal shifts will be investigated.~~ biology.

Schimanke and Meier (2016) analyzed multidecadal variations in Baltic Sea salinity and the coherence with different physical drivers. They used the wavelet transform to identify periodicities and wavelet coherency to analyse the driving mechanisms.

## 2 Methods

### 2.1 Study area

The Baltic Sea contains several different sub-basins with different characteristics in salinity and nutrient loads. We have here chosen to focus on the Baltic Proper. To obtain homogenous conditions we focus on the open ocean away from coasts. Areas where the depth is less than 20m are therefore removed. The study area is displayed in Fig. 1.

We have chosen to use a basin ~~integrated~~ averaged approach. All variables have thus been horizontally ~~integrated~~ averaged over the study area. This way we ~~aim to gain an~~ remove local variability and hope to gain a better understanding of the ~~overall functioning of the~~ system.

### 2.2 Model

We have used a run with the model RCO-SCOBI spanning 1850-2009. RCO (Rossby Centre Ocean model) is a three-dimensional regional ocean circulation model(Meier et al., 2003). It is a z-coordinate model with a free surface and an open boundary in the northern Kattegat. The version used here has a horizontal resolution of 2nm with 83 depth levels at 3m intervals.

The biogeochemical interactions are solved by the Swedish Coastal and Ocean Biogeochemical model (SCOBI) (Eilola et al., 2009; Almroth-Rosell et al., 2011)~~is a one dimensional biogeochemical model that~~. The model solves for three different water column and benthic nutrients (phosphate, nitrate and ammonia) as well as plankton functional types representing diatoms, flagellates and others (will be referred to as flagellates from here on) and cyanobacteria. Furthermore, the model contains nitrogen and phosphorus in one active homogenous benthic layer.

The model equations can be found in Eilola et al. (2009). Since we are exploring the effect of different variables on the growth of phytoplankton we will, for clarity, repeat some of them here.

The ~~time rate of change of the concentration of phytoplankton chlorophyll in units of mg Chl m$^3$ day$^{-1}$ is described by~~

88 $\mathrm{S_{PHY}} \quad = \quad \mathrm{GROWTH_{PHY} + NFIX + SINKI_{PHY}}$

89 $\qquad \qquad \quad \mathrm{-SINKO_{PHY} - MORT_{PHY} - GRAZE_{PHY},}$

90 ~~where subscript PHY stands for phytoplankton 1 (diatoms), 2 (flagellates) or 3 (cyanobacteria). $\mathrm{GROWTH_{PHY}}$ describes the~~

91 ~~growth of phytoplankton, NFIX the production by nitrogen fixation, $\mathrm{SINKI_{PHY}}$/$\mathrm{SINKO_{PHY}}$ the flux of phytoplankton into /out~~

92 ~~of the current layer, $\mathrm{MORT_{PHY}}$ the mortality and $\mathrm{GRAZE_{PHY}}$ grazing by zooplankton~~phytoplankton biomass is described in

93 terms of chlorophyll and with a constant C:Chl ratio. The model thus does not take into account seasonal changes in C:Chl as

94 was found by Jakobsen and Markager (2016) .

95 The net growth of phytoplankton is described by the following expression,

96 $\mathrm{GROWTH_{PHY}} \quad = \quad \mathrm{ANOX \cdot LTLIM \cdot NUTLIM_{PHY} \cdot GMAX_{PHY} \cdot PHY,}$ \hfill (1)

97 where subscript PHY indicates the plankton funktional type (diatoms, flagellates or cyanobacteria). ANOX is a logarithmic

98 expression that approaches zero as the oxygen concentration becomes small. ~~ANOX also contains a switch that sets it equal to~~

99 ~~zero when the oxygen concentration is zero so that no phytoplankton growth can occur in anoxic environments.~~

100 LTLIM expresses the phytoplankton light limitation and NUTLIM describes the nutrient limitation. Nutrient limitation

101 follows Michaelis-Menten kinetics where constant Redfield ratios are assumed in nutrient uptake. NUTLIM ~~and LTLIM~~ is

102 further described in Sects. 2.2.1 and 2.2.2. GMAX is temperature dependent and describes the maximum phytoplankton growth

103 rate.

104 The difference between diatoms and flagellates are present in halfsaturation constants, maximum growth rate, temperature

105 dependence and sinking rate. Flagellates are more sensitive to a change in temperature than diatoms. Furthermore, the sinking

106 rate of diatoms is five times larger than that for flagellates.

107 The difference between cyanobacteria and the other phytoplankton species is more pronounced. Cyanobacteria can grow

108 either according to Eq. (1) or using nitrogen fixation~~according to~~

109 $\mathrm{NFIX} \quad = \quad \mathrm{ANOX \cdot NF \cdot A3}$

110 ~~where NF is the~~ . The rate of nitrogen fixation as a function of the phosphate concentration and temperature~~, and A3 is the~~

111 ~~concentration of cyanobacteria~~. Both NFIX and GROWTH of cyanobacteria is zero if the salinity is above 10. Furthermore,

112 cyanobacteria is the most temperature sensitive of the phytoplankton groups and no sinking velocity is assumed.

113 Other processes important for our results involves chemical reactions occurring in the water column or in the sediment.

114 Denitrification occurs in both the water column and the benthic layer and constitutes a sink for nitrate in case of anoxia.

115 Nitrification transforms ammonium into nitrate as long as oxygen is present. Phosphorus is adsorbed to the sediment and the

116 benthic release capacity of phosphate is a function of the oxygen concentration where more oxygen implies less release. The

117 phosphorus release capacity is also dependent on salinity where higher salinity means ~~more~~ less phosphate is retained in the
118 benthic layer.

### 2.2.1 Nutrient limitation

120 Estimating nutrient limitation in nature is difficult. Usually this is done, either by comparing nutrient ratios to Redfield in eg.
121 the surface water or external supply or by some nutrient enrichment experiment (Granéli et al., 1990).

122     The idea of nutrient limitation as often used is based on that the primary production is directly limited by the nutrient
123 concentration in the ambient water and that the internal nutrient ratios in the phytoplankton are constant, i.e. in accordance with
124 a Redfield-Monod model (Redfield, 1958). However, cell-quota type models (Droop, 1973) are being increasingly implemented
125 and the use of constant internal nutrient ratios are becoming more and more questioned (Flynn, 2010).

126     Furthermore, N vs P limitation is a long standing debate. Tyrrell (1999) uses a box-modelling approach to show that in
127 steady state, nitrogen becomes slightly deficient while it is the external input and removal of phosphate that ultimately controls
128 the production.

129     Here, nutrient limitation is traditionally expressed assuming constand Redfield ratios and phytoplankton growth is limited
130 by either nitrogen or phosphate. The degree of nutrient limitation is described by:

$$131 \quad \mathrm{NUTLIM_{PHY}} \quad = \quad \min(\mathrm{NLIM_{PHY}}, \mathrm{PLIM_{PHY}}) \tag{2}$$

132 where $\mathrm{NLIM_{PHY}}$ and $\mathrm{PLIM_{PHY}}$ are the nitrogen and phosphate limitation respectively. In addition, $\mathrm{NLIM_{PHY}}$ contains the
133 sum of the nitrate and ammonium limitation, i.e.

$$134 \quad \mathrm{NLIM_{PHY}} \quad = \quad \mathrm{NO_3LIM_{PHY}} + \mathrm{NH_4LIM_{PHY}}, \tag{3}$$

135 where

$$136 \quad \mathrm{NO_3LIM} \quad = \quad \frac{\mathrm{NO3}}{\mathrm{KNO3_{PHY}} + \mathrm{NO3}} \cdot \exp(-\phi_{\mathrm{PHY}} \cdot \mathrm{NH_4}), \tag{4}$$

$$137 \quad \mathrm{NH_4LIM} \quad = \quad \frac{\mathrm{NH4}}{\mathrm{KNH4_{PHY}} + \mathrm{NH4}}, \tag{5}$$

138 where NO3 and NH4 are the concentrations of nitrate and ammonium and $\mathrm{KNO3_{PHY}}$ and $\mathrm{KNH4_{PHY}}$ are the halfsaturation
139 constants for nitrate and ammonium respectively. The exponent in (4) ~~represents preferential ammonium~~ accounts for inhibition
140 of nitrate uptake (eg. Dortch (1990); Parker (1993)).

141     $\mathrm{PLIM_{PHY}}$ is modelled as,

$$142 \quad \mathrm{PO_4LIM} \quad = \quad \frac{\mathrm{PO4}}{\mathrm{KPO4_{PHY}} + \mathrm{PO4}}. \tag{6}$$

143  Nutrient limitation is thus described by a number between 0 and 1 where 1 is no limitation. Note that NLIM in Eq. (3) may

144  obtain values larger than 1. However, as NUTLIM is calculated as the minimum of NLIM and PLIM, NLIM larger than one

145  will always mean P limitation.

146  The constants $KNO3_{PHY}$, $KNH4_{PHY}$ and $KPO4_{PHY}$ are the half saturation constants and differs between the different

147  phytoplankton groups. The constant $\phi_{PHY}$ in Eq. (4) determines the strength of ammonium inhibition of nitrate uptake. The

148  values of the constants for each phytoplankton type are given below.

149  $$KNO3_{PHY} \equiv 0.5/0.25/0.25$$

150  $$KNH4_{PHY} \equiv 0.5/0.25/0.25$$

151  $$KPO4_{PHY} \equiv 0.1/0.05/0.05$$

152  $$\phi_{PHY} \equiv 1.5/1.5/1.5$$

153  Note that the half-saturation constants for flagellates and cyanobacteria are equal which means that in absence of nitrogen

154  fixation, the nutrient limitation for the nitrogen fixing species is equal to that of flagellates.

155  In addition to the above given nutrient limitation of phytoplankton growth there exists a similar nutrient dependency on

156  nitrogen fixation. In the model this dependency reads

157  $$NUTLIM_{NF} \equiv \frac{aNFC}{aNFC + \left(\frac{NO_3 + NH_4}{PO_4 cNFC} dNFC\right)}) \cdot \frac{PO_4}{\alpha NF \cdot \beta NF + PO_4},$$

158  where aNFC, bNCF, cNFC and dNFC are constants used for calculating the nitrogen fixation capacity which in turn is a

159  function of the ratio of inorganic nitrogen to phosphate. $\alpha NF$ and $\beta NF$ are constants determining the half-saturation for nitrogen

160  fixation. Again, $NUTLIM_{NF}$ approaches one if the nitrate and ammonium concentrations are zero and for large concentrations

161  of phosphate.

162  ### 2.2.2  Effect of physical parameters

163  Changes in cloud-cover affect the incoming solar radiation and thereby the phytoplankton growth. The effect of light shows up

164  in the LTLIM term of Eq. (1).

$$165 \quad \underline{\text{LTLIM}} \quad \equiv \quad \underline{\text{fracI}_{\text{PAR}}\text{I}_{\text{opt}} \cdot \text{EXP}\left(1 - \frac{\text{I}_{\text{PAR}}}{\text{I}_{\text{opt}}}\right),}$$

$$166 \quad \underline{\text{I}_{\text{PAR}}(\text{z})} \quad \equiv \quad \underline{\alpha_{\text{PAR}}\text{I}_0 \cdot \text{EXP}\left(-\text{Kd} \cdot \text{z}\right)}$$

$$167 \quad \underline{\text{I}_{\text{opt}}} \quad \equiv \quad \underline{\max(\text{I}_{\text{opt,min}}, \alpha_{\text{opt}}\text{I}_0)}$$

$$168 \quad \underline{\text{Kd}} \quad \equiv \quad \underline{\text{Kd}_{\text{w}} + \text{Kd}_{\text{PHY}} + \text{Kd}_{\text{Y}} + \text{Kd}_{\text{D}}}$$

$$169 \quad \underline{\text{Kd}_{\text{PHY}}} \quad \equiv \quad \underline{\alpha_{\text{Kd}}(\text{A1} + \text{A2} + \text{A3})}$$

170 ~~where $I_{PAR}$ is the photosynthetic available radiation and $I_{opt}$ is the optimum irradiance for phytoplankton growth. $I_{opt,min}$ is~~

171 ~~a constant minimum optimum irradiance, $I_0$ is the surface irradiance and Kd is the vertical attenuation. $Kd_w$ is the background~~

172 ~~attenuation, $Kd_{PHY}$ is the light attenuation due to the concentration of phytoplankton, $Kd_Y$ the attenuation due to humic~~

173 ~~substances (calibrated) and $Kd_D$ the attenuation due to detritus. $\alpha_{Kd}$ is a constant vertical attenuation per unit chlorophyll.~~

174 ~~A1/2/3 is the concentration of the respective phytoplankton type.~~

175    The mixed layer depth has been defined as the depth where a density difference of $0.125 \, \text{kg m}^{-3}$ from the surface is reached

176 in accordance with what was previously done by e.g. Eilola et al. (2013). The density was calculated from modelled temperature

177 and salinity using the ~~matlab routines by~~ algorithms from Jackett et al. (2006).

## 2.3  Forcing

179 The study use reconstructed (1850-2008) atmospheric, hydrological and nutrient load forcing and daily sea levels at the lateral

180 boundary as described by Gustafsson et al. (2012) and Meier et al. (2012). Monthly mean river flows were merged from

181 reconstructions done by Hansson et al. (2011) and by Meier and Kauker (2003) and hydrological model data by Graham

182 (1999), respectively. For further details about the physical model setup used in the present study the reader is referred to Meier

183 et al. (2016) and references therein.

184    The nutrient loads from rivers and point sources were (1970-2006) compiled from the Baltic Environmental and HELCOM

185 databases (Savchuk et al., 2012). Estimates of pre-industrial loads for 1900 were based upon Savchuk et al. (2008). The

186 nutrient loads were linearly interpolated between selected reference years in the period between 1900 and 1970. Similarly,

187 atmospheric loads were estimated (Ruoho-Airola et al., 2012). Nutrient loads contain both organic and inorganic phosphorus

188 and nitrogen, respectively. For riverine organic phosphorus and nitrogen loads bioavailable fractions of 100 and 30% are

189 assumed, respectively.

190    Figure 2 shows the loads of Dissolved Inorganic Phosphorus (DIP, top) and Dissolved Inorganic Nitrogen (DIN, bottom)

191 to the Baltic Proper as ~~used in the model~~ defined in Fig. 1. The loads are shown together with the corresponding simulated

192 mixed layer concentration. The loads are calculated from the runoff and annual mean nutrient concentrations (Eilola et al.,

193 2011). Thus the seasonal cycle in river loads is determined by the runoff. After a spin-up simulation for 1850-1902 utilizing

194 the reconstructed forcing as described above, the calculated physical and biogeochemical variables at the end of the spin-up

195 simulation were used as initial condition for 1850.

The open boundary conditions in the northern Kattegat were based on climatological (1980-2000) seasonal mean nutrient concentrations (Eilola et al., 2009). ~~The bioavailable fraction of organic phosphorus was assumed to be 100% in accordance with the phosphorus supply from land runoff.~~ Similar to Gustafsson et al. (2012) a linear decrease of nutrient concentrations back in time was added assuming that climatological concentrations in 1900 amounted to 85% of present day concentrations (Savchuk et al., 2008). The bioavailable fraction of organic phosphorus at the boundary was assumed to be 100% in accordance with the organic phosphorus supply from land runoff. Organic nitrogen was implicitly added because of the Redfield ratio of model detritus (Eilola et al., 2009).

## 2.4 The wavelet transform and wavelet coherence

Several references explain the wavelet transform and its application in depth (e.g. Lau and Weng (1995), Torrence and Compo (1998), Carey et al. (2016), Grinsted et al. (2004)) and we will here provide a brief introduction.

The continuous wavelet transform provides a method to decompose a signal into time-frequency space. In ~~contrast to the Fourier transform, the wavelet decomposition thus provides time localization and the means to see how periodicities change with time. Wavelet coherence further expands the usefulness of the approach by allowing for calculating the time resolved coherence between two~~ that it is similar to the windowed Fourier transform where the signal is decomposed within a fixed time-frequency window which is then slided along the time-series. ~~For all wavelet calculations we use the Matlab wavelet package of described in Grinsted et al. (2004), which is freely available at http://www. glaciology. net/wavelet-coherence.~~ However, the fixed width of the window leads to an underestimation of low frequencies. In comparison, the wavelet transform utilizes wavelets with a variable time-frequency window. Wavelets can have many different shapes and the choice is not arbitrary. We have chosen the commonly used Morlet wavelet providing good time and frequency localization (Grinsted et al., 2004).

In time-series with clear periodic patterns that is affected by environmental variables such as population dynamics and ecology the benefits with this approach are significant (Cazelles et al., 2008). ~~Several studys have implemented wavelet analysis to plankton dynamics. Winder and Cloern (2010) applied the technique to time-series of chlorophyll-a from different localities and discussed the annual and seasonal periodicities~~ In recent years, several references have highlighted the usefulness of wavelet analyses in plankton research (Winder and Cloern, 2010; Carey et al., 2016). The focus have been the increased availability of long observational data sets making it possible to use the wavelet transform for investigation of changes in seasonality. Carey et al. (2016) discussed how the wavelet transform can be used to track interannual changes in phytoplankton biomass and applied it to a 16-year time series of phytoplankton in Lake Mendota, USA. In doing this they were able to identify periods when the annual periodicity was less pronounced. They discuss the benefit of this technique in scrutinizing changes to the seasonal succession due to changes in external drivers. Winder and Cloern (2010) applied the technique to time-series of chlorophyll-a from marine and freshwater localities and discussed the annual and seasonal periodicities.

Wavelet coherence further expands the usefulness of the wavelet approach by allowing for calculating the time resolved coherence between two time-series (Grinsted et al., 2004; Cazelles et al., 2008). In this way, it is possible to identify transient

229 periods of correlation over different periodicities. The result is given as coherency as a function of time and period as well as a
230 phase lag between the two time-series.

231 The problem with the wavelet transform is that it requires a dataset without gaps. The time-series also needs to be sufficiently
232 long compared to the investigated periods. This makes it difficult to use the method to scrutinize the ~~effect~~ coherence of
233 processes acting on longer time-scales, such as climate change, since long enough observational datasets are scarce. Hence, for
234 our purpose only a model based approach is feasible.

235 ~~Here we use wavelet coherence to~~ Schimanke and Meier (2016) used wavelet coherency on a multi-centennial model run to
236 evaluate the correlation of different forcing variables with the Baltic Sea salinity. We will here scrutinize the coherence between
237 ~~the three different phytoplankton groups (diatoms, flagellates, and cyanobacteria) and nutrients, temperature, irradiance and~~
238 ~~mixed layer depth~~ modelled phytoplankton biomass and a few key modelled and forcing variables.

239 For all wavelet calculations we use the Matlab wavelet package of described in Grinsted et al. (2004) , which is freely
240 available at http://www.glaciology.net/wavelet-coherence.

**2.5** ~~Observations~~

242 ~~Oxygen and nutrient concentrations from the SCOBI model have been extensively evaluated against observations (Eilola et al., 2009, 2011,~~
243 ~~well as other models (Eilola et al., 2011) . Phytoplankton observations are more difficult to come by and our basin integrated~~
244 ~~approach makes it difficult to compare with observations from individual stations.~~

245 ~~We have used a basin integrated dataset of monthly Chl-a for the Baltic Proper previously published in HELCOM (2012) .~~
246 ~~The dataset includes all data from the Data Assimilation System (DAS) which is a database of Baltic Sea monitoring data~~
247 ~~hosted by the Baltic Nest Institute, Stockholm University, completed with data from the EUTRO-PRO project and HELCOM~~
248 ~~Indicator Fact Sheets (HELCOM, 2012) .The surface layer was defined as the top 10m of the water column and coastal areas~~
249 ~~were removed.~~

**3 Results and discussion**

251 The ~~model~~ results shown are monthly means ~~integrated~~ averaged over the basin. The different variables have also been vertically
252 ~~integrated~~ averaged over the mixed layer and/or from the mixed layer down to a depth of 150m. ~~The first 20 yrs of the model~~
253 ~~run is exluded to minimize spinup effects.~~

254 We ~~start out~~ will begin in Sect. 3.1 by ~~scrutinizing the modelled concentration of phytoplankton and its seasonal cycle by~~
255 ~~comparison with observations. In Sect. 3.3, the coherence between nutrient loads and mixed layer nutrient concentrations as~~
256 ~~well as phytoplankton concentrations will be examined. Section 3.2~~ presenting the model results of phytoplanton biomass.
257 In Section 3.2 we will consider the composition of nutrients and ~~its effect on the phytoplankton concentrations. The effect~~
258 ~~of temperature and irradiance is scrutinized~~ the coherence with the phytoplankton biomass. Coherence between riverine
259 loads and mixed layer nutrients will be discussed in Sect. ~~3.4 and in Sect. 3.5~~ 3.3. Section 3.4 examines the coherence of

260 the phytoplankton with temperature and irradiance. Finally, the coherence between mixed layer depth with phytoplankton is

261 examined. and phytoplankton biomass is considered in Sect. 3.5.

## 3.1 Phytoplankton - model and observationsbiomass

Figure ?? shows the model results of basin integrated Chl-a concentration (the sum of the three different phytoplankton )
over 0-10m Fig. 3 shows the time-series of phytoplankton biomass (a) together with the observations described above. The
results are thus here integrated over a fixed depth rather than the mixed layer to better compare with the observations. The top
panel of Fig. ?? displays observations and model results for the period 1990-2009. In order to illustrate the difference from
pre-industrial, model results for the period 1880-1999 are also shown. corresponding wavelet spectrum (b).

The top panel reveals that the largest values representing the spring bloom are underestimated in the model results compared
to the observations. The model implements a constant C:Chl ratio of 50 in phytoplankton, while Jakobsen and Markager (2016) found
that this ratio, in reality, varies throughout the year. The underestimation of the spring bloom in the model may therefore, at
least in part, be explained by this simplified assumption. Furthermore, the wavelet transform reveals a strengthening in the
model of The wavelet power (variance) of the 6 month period relative to the annual compared to the early period (panel (c) and
(d))decomposed signal (in color) is displayed as a function of time (x-axis) and period (y-axis). The black curves in Fig. ??) .
This is caused by the large increase in cyanobacteria resulting in a stronger late summer bloom. The half year period is much
weaker in the observations. In the upper panel of Fig. ??, this is visable as a greater observed difference between 3(b) show the
95% confidence level relative to red noise.

Averaging over time generates the global power spectrum displayed in Fig. 3 (c). The wavelet spectrum clearly reveals two
main periodicities - the annual and the semi-annual representing the spring and late summer blooms. The smaller difference in
magnitude between the two blooms in the model results reflects as stronger signal with a 6 month periodicity in the wavelet
spectrum (panel (c) in Fig. ??). autumn blooms. It is also clearly visable that the power on both periodicities increases markedly
after 1950.

Kahru et al. (2016) found a shift in chlorophyll maxima from the diatom dominated spring bloom to the cyanobacteria
summer bloom. Fig. 4 shows that a similar pattern emerges from our model run with five years of cyanobacterial chlorophyll
maxima occurring after 1998.

## 3.2 Nutrient loads

To determine the effect of the riverine loads on the mixed layer nutrient concentrations we perform wavelet coherence. The
result is shown in Fig. 12. We have used riverine DIN and DIP loads in the results presented below. The use of instead total
bioavailable nutrient loads does not change the results.

The results show the clear annual cycle in riverine inputs and mixed layer nutrient concentrations. The phosphate loads show
little coherence on any other periodicity but DIN displays strong coherence on longer periods. Furthermore, there is a tendency
for a enhanced coherence during the later part of the run most likely caused by increased DIN loads.

292 The phase arrows on the annual scale points to the right during most of the run indicating that the seasonal peak in nutrient
293 loads and mixed layer concentrations are concurrent. However, during the period 1900-1920 the direction of the phase arrows
294 shifts upwards. This is a result of a persistent shift in the runoff maxima of about two months over the period. During this
295 period the peak in mixed layer nutrient concentrations thus precedes the runoff peak. The interpretation of this is not straight
296 forward but most probably it has to do with the scarcity of observations and the use of an integrated Baltic Sea runoff dataset

## 3.2 Nutrients and nutrient limitation

298 The extent of anoxic bottoms in the Baltic Sea has increased markedly over the past century. Carstensen et al. (2014) found
299 a 10-fold increase in the hypoxic area since the beginning of the 20th century. They explained this to be primarily due to
300 increased nutrient loads causing increased primary production and resulting in an enhanced deep water respiration.
301 To further investigate the lack of inter-annual coherence between riverine phosphate loads and mixed layer phosphate, the
302 wavelet coherence between mixed layer salinity and nutrients are examined and displayed in Fig.13. Mixed layer salinity is
303 affected by freshwater input from land, precipitation, evaporation and mixing with deeper layers. The coherence spectrum
304 reveals higher coherence between mixed layer salinity and phosphate (top) on interannual periodicities than between salinity
305 and DIN (bottom) Changing nutrient patterns in the Baltic Sea due to spreading hypoxia have been discussed by e.g. Conley et al. (2002); Sa
306 Anoxia causes sedimentary phosphate release. A clear relationship between hypoxia and total basin averaged phosphate was
307 first shown by Conley et al. (2002) (and later expanded by Savchuk (2010) ) on observational data from the Baltic Proper.
308 The effect of hypoxia on DIN is less straight forward. Expanding hypoxia increases the boundary area between anoxic
309 and oxic water where denitrification occurs resulting in a further loss of nitrate. Furthermore, hypoxia induced reduction in
310 nitrification results in a loss of nitrate. Vahtera et al. (2007) found a negative relationship between basin averaged DIN and
311 hypoxic area in observations from the Baltic sea. The coherence existing between salinity and DIN on periodicities longer than
312 one year is antiphase i. e. low salinity here coheres with high DIN concentrations. In contrast, the in-phase coherence between
313 salinity and phosphate suggests that the reason for the coherence is a greater importance of the internal source i. e. phosphorus
314 release from the sediments that eventually reaches the mixed layer through mixing with deeper layers.
315 Figures ?? and ?? show the coherence between the riverine input of phosphate/DIN and mixed layer chl concentrations of
316 diatoms (top), flagellates (middle) and cyanobacteria (bottom). There is again a strong annual coherence. There seems to be
317 a quite strong coherence between mainly diatoms and both nutrients on a 16 year period. However, given that the length We
318 illustrate the changing nutrient patterns for our model run in Fig. 5. In conjunction with the increased anoxic volume we find a
319 clear increase in ammonium and a decrease in nitrate. This is due to a decrease in nitrification and an increase in denitrification.
320 The phosphate concentration increases from the mid 20th century through the rest of the model run does not even give room
321 for ten 16-year periods, this probably reflects the overall pattern of simultaneous increase in riverine loads and chlorophyll
322 concentrations over the second half of the 20th century as a combined effect of the accumulated terrestrial inputs and hypoxic
323 sedimentary release.

## 3.3 Nutrients and nutrient limitation

325 ~~We will here assess the coherence of nutrients with the phytoplankton concentrations. Furthermore, as described above, the~~ The

326 effect of nutrients on the primary production is in the model controlled by the term NUTLIM, or degree of nutrient limitation,

327 in Eq. (1). ~~We thus~~ NUTLIM can be viewed as a measure of the nutrient composition that linearly affects the phytoplankton

328 growth in the model. We will examine this term in and below the mixed layer. Even though there is no primary production in

329 the deep water and thus the nutrient limitation term has no effect here, a shift in the composition of nutrients in the deep water

330 will affect also the mixed layer. NUTLIM for ~~the different plankton groups~~ diatoms and flagellates has been calculated offline

331 from the monthly means according to ~~Eqs~~ Eq. (2)~~and (7~~.

332 The evolution of NUTLIM in the surface layer and the deep water for diatoms and flagellates is shown in Fig. 6. There is a

333 clear increase over the 20th century and a shift towards less limited conditions (NUTLIM approaching 1).

334 Nitrogen has been shown to most often be limiting in the Baltic Proper, while phosphate is limiting in the northern

335 basins (Granéli et al., 1990; Tamminen and Andersen, 2007). ~~However~~ Schernewski and Neumann (2004) showed through a

336 reconstruction of the Baltic Sea trophic state in the early 1900 that N/P ratios in the Baltic Proper have decreased but that much

337 of the domain still indicated N limitation.

338 Using the models definition of nutrient limitation, our model results, ~~displayed~~ shown in Fig. 7, ~~show~~ display phosphate

339 limitation for both diatoms and flagellates for the earlier part of the run. After 1980, seasonality appears in the mixed layer.

340 Phosphate is still limiting during winter while nitrogen becomes limiting after the spring bloom. Calculating N/P ratios as

341 a more conventional measure of nutrient limitation, our model results diplay instead a shifting pattern until 1976 whereafter

342 persistant N limitation develops (not shown).

343 ~~The extent of anoxic bottoms in the Baltic Sea has increased markedly over the past century. By compilation of a large~~

344 ~~amount of temperature, salinity and oxygen observations Carstensen et al. (2014) found a 10-fold increase in the hypoxic area~~

345 ~~since the beginning of the 20th century. They explained this to be primarily due to increased nutrient loads from land causing~~

346 ~~increased deep water respiration but also due to increased temperatures resulting in reduced oxygen solubility.~~

347 ~~In order to understand the limitationpatterns found in our model run, we view the evolution of different nutrient concentrations.~~

348 ~~Figure 5 shows the anoxic volume together with the below mixed layer nutrient concentrations. In conjunction with the~~

349 ~~increased anoxic volume we find a clear increase in ammonium concentration. This is due to a decrease in nitrification and~~

350 ~~is seen also as a decrease in the nitrate concentration. Furthermore, expanding anoxic bottoms increase the boundary area~~

351 ~~between anoxic and oxic water where denitrification occurs resulting in a further loss of nitrate.~~

352 ~~Figure 5 also shows that the phosphate concentration increases from the mid 20th century through the rest of the model run.~~

353 ~~This is a combined effect of increased riverine loads and enhanced sedimentary release due to anoxia.~~

354 ~~The mixed layer displays corresponding patterns of increased phosphate and decreased nitrogen (Fig. ??). The seasonal~~

355 ~~variations are however much greater since the majority of the primary production occurs here and since the mixed layer is~~

356 ~~directly affected by riverine input. The mixed layer also comprises a smaller volume of water. Despite quite high wintertime~~

357 ~~concentrations, the spring bloom almost completely depletes the nitrogen. The seasonality that appears after 1980 in mixed~~

358 ~~layer nutrient limitation with nitrogen limitation after the spring bloom is thus a results of the larger relative increase in~~

359 ~~phosphate compared to nitrogen.~~

**12**

360    ~~The sum of the effects on the nutrient concentrations shows up in the nutrient limitation expressions (Eqs. (3)-(6)).~~

361    ~~The evolution of NUTLIM in the surface layer and the deep water for the three phytoplankton is shown in Fig. 6. There~~

362    ~~is a clear increase over the 20th century and a shift towards less limited conditions~~The changing nutrient patterns affects the

363    phytoplankton growth. We analyse the wavelet coherencies of phytoplankton biomass with mixed layer phosphate and DIN in

364    Figs. 8 and 9.

365    ~~After 1980 there is a shift in the variability of nutrient limitation for diatoms and flagellates most clearly visible in the deep~~

366    ~~water. This shift is also visible in the lower two panels of Fig. 7 which show that deepwater NUTLIM shifts towards a purely~~

367    ~~nitrogen limited regime while NUTLIM for flagellates mostly display a seasonal pattern. The lower variability is due to the~~

368    ~~characteristics of the nitrogen limitation Eq. (3) . The concentrations of nitrate and ammonium at the end of the model run~~

369    ~~corresponds to a minimum in Eq. (3). Therefore, even though the concentrations change, NUTLIM changes very little.~~

370    ~~To see how the phytoplankton concentrations are connected to nutrient concentrations and nutrient limitation, we continue~~

371    ~~by scrutinizing the wavelet coherencies.~~

372    ~~Figure 8 and 9 show the wavelet coherencebetween mixed layer phosphate and DIN and phytoplankton. Diatoms which~~

373    ~~are the most~~ Coherency is shown in color as a function of year (x-axis) and period (y-axis). More yellow indicates stronger

374    coherence. The arrows reveal the phase-lag between the two time-series. The line plots on the right show the time averaged

375    coherence. As the strongest nutrient limited group~~show strong~~, diatoms show persistant inter-annual coherence with phosphate

376    during the first, consistently phosphate limited part of the run (see Fig. 7). During the later part of the run the nutrient and

377    phytoplankton concentrations are ~~so high~~ high enough that smaller inter-annual variations have little effect.

378    Since nitrogen limitation in the model only occurs after 1980 and after the spring bloom and thus only affects the much

379    smaller diatom and flagellate autumn blooms no coherence between phytoplankton and nitrogen is visable in Fig. 9.

380    ~~To further illustrate the shift from the more nutrient limited regime of the first part of the run we calculate the wavelet~~

381    ~~coherence between NUTLIM for the different phytoplanktonand the result is displayed in Fig. ??. Again, diatoms show strong~~

382    ~~coherence during the first, more nutrient limited part of the run.~~

383    ~~In Fig. 10~~ To scrutinze the shift in deep water nutrient composition and the coherence with phytoplankton, we calculate the

384    wavelet coherence between below mixed layer NUTLIM and the ~~three types of phytoplankton. Again, the coherence spectrum~~

385    ~~shows the most inter-annual coherence for the more nutrient limited diatoms. However, the phase arrows~~ diatom and flagellate

386    biomass. The result is shown in Fig. 10. The phase arrows here display some interesting features. After 1980 the phase arrows

387    within the annual coherence period change ~~direction~~to the opposite direction. For diatoms, the phase shifts from NUTLIM

388    preceding diatoms by three months to diatoms preceding nutlim by the same amount. Flagellates display a similar shift. ~~This~~

389    ~~occurs both for diatomswhere they shift from downward, indicating that the annual NUTLIM periodicity precedes the annual~~

390    ~~diatom periodicity by 90 degrees, i.e. 3 months , to upwards, instead indicating that the diatoms precedes NUTLIM. A similar~~

391    ~~pattern is visable also in flagellates.~~

392    To investigate ~~the reasons for~~ this, we have plotted the month of maximum NUTLIM in Fig. 11. The figures show a clear

393    shift occuring after ~~1980 correlating with a strengthening of cyanobacteria blooms. The deep water~~ 1980. Below the mixed

394    layer, NUTLIM changes its maxima ~~to the late summer months~~ from December and January to July, August and September

**13**

while a slight shift from February to March is apparent for diatoms. Mixed layer NUTLIM for flagellates displays no clear shift.

Figure 4 shows the timing of the maximum chlorophyll concentration for the different phytoplanktons as well as their sum. Flagellates displays a weak shift towards May after 1960 but no other shifts are visable in the individual phytoplankton types. However, the total chlorphyll concentration (Diatoms + Flagellates + Cyanobacteria) displays a few years at the very end of the run where the chlorophyll maximum corresponds to the maximum for cyanobacteria. From satellite data, Kahru et al. (2016) found a similar shift in chorophyll maximum from the spring bloom in May to the cyanobacteria bloom in July

## 3.3 Nutrient loads

The wavelet coherence between mixed layer nutrients and riverine input is shown in Fig. 12. We have used riverine DIN and DIP loads in the results presented below. The use of instead total bioavailable nutrient loads does not change the results.

The phosphate loads show little coherence on periodicities longer than one year but DIN displays strong inter-annual coherence. The phase-arrows indicate a phase-lag of about minus $45°$ on all inter-annual periodicities. For an 8 year period this means that riverine input precedes DIN by about 1 yr.

To further investigate the lack of inter-annual coherence between riverine phosphate loads and mixed layer phosphate, the wavelet coherence between mixed layer salinity and nutrients are examined and displayed in Fig. 13. Mixed layer salinity is affected by freshwater input from land, precipitation, evaporation and mixing with deeper layers. The coherence spectrum reveals higher coherence between mixed layer salinity and phosphate (top) on interannual periodicities than between salinity and DIN (bottom). The coherence existing between salinity and DIN on periodicities longer than one year is antiphase i.e. low salinity here coheres with high DIN concentrations. In contrast, the in-phase coherence between salinity and phosphate suggests that the reason for the coherence might be a greater importance of phosphorus release from the sediments that eventually reaches the mixed layer through mixing with deeper layers.

Riverine nutrient loads show little inter-annual coherence with phytoplankton biomass (not shown) other than on a 16 yr period which probably reflects the overall pattern of simultaneous increase in riverine loads and phytoplankton biomass over the second half of the 20th century.

## 3.4 Temperature and irradiance

The mixed layer temperature has increased over the 20th century. Figure 14 shows the 2-yr moving average of mixed layer temperature. To scrutinize the effect of temperature on the concentration of phytoplankton, the wavelet coherence between temperature and phytoplankton have been plotted in Fig. 15. The results suggest that the temperature increase after 1990 might have had an effect on cyanobacteria and flagellates. It is also noticeable that the temperature increase observed between 1900 and 1940 probably had an effect on cyanobacteria. This is also in agreement with the model formulation where cyanobacteria are the most sensitive to temperature followed by flagellates.

14

Light impacts primary production through the term LTLIM in Eq. (1). However, irradiance display very little variation on any other periodicity than the annual as can be observed in a wavelet power spectrum (not shown). Therefore there exists almost no coherence between phytoplankton and irradiance apart from the annual and semiannual.

## 3.5 Mixed layer depth

The lower panel of Fig. 14 shows the two year moving average of mixed layer depth averaged over the basin. We calculate the coherence between mixed layer depth and diatoms, flagellates and cyanobacteria in Fig. 16.

Apart from the annual cycle there is a strong coherence between mixed layer depth and diatoms, and to some extent flagellates, on shorter periodicities as well. That is, the concentration of diatoms residing in the mixed layer seems to covary quite well on periodicities equal to or shorter than one year. The model value for diatom sinking rate is five times higher than that for flagellates while cyanobacteria is assumed to have no sinking rate. In a shallow mixed layer the diatom concentration decreases faster than in a deep mixed layer because of the large sinking rate. In the wavelet coherence spectrum we thus see in-phase short term coherence.

## 4 Summary and conclusions

With a ~~main~~ focus on inter-annual variations, the coherence of the mixed layer ~~concentrations of phytoplankton~~ phytoplankton biomass with key variables affecting the primary production has been examined for the Baltic Proper.

~~Riverine input of nutrients is an extremely important variable in the Baltic Sea and the large increase during the 20th century has initiated spreading of anoxic bottoms (Carstensen et al., 2014) . We found quite strong coherence between riverine input of DIN and mixed layer DIN but not a similar relationship between riverine phosphate input and the corresponding mixed layer concentration. As mixed layer salinity displayed in-phase inter-annual coherence with phosphate and only weak anti-phase coherence with DIN we conclude that this is most probably due to a greater importance of the internal source of phosphate from lower layers.~~

~~We further found that the~~ We found that the pattern of nutrient limitation in and below the mixed layer have changed in the model since 1980. Below the mixed layer, the limitation pattern changes from phosphate to nitrogen for diatoms and to seasonally shifting between phosphate and nitrogen. Within the mixed layer, the pattern changes from pure phosphate limitation to seasonally shifting for both diatoms and flagellates. This is due to decreased deep water oxygen concentrations and a rapid expansion of anoxia after 1970. The phosphate concentrations increase due to enhanced sedimentary release, denitrification results in loss of nitrate and reduced nitrification decreases the transformation of ammonium to nitrate. The combined effect results in nitrogen limitation after the spring bloom which benefits cyanobacteria.

The mixed layer concentrations of nutrients affect the primary production in the model through the nutrient limitation term, NUTLIM. The phytoplankton group most strongly limited by nutrients in the model is diatoms. The connection between primary production and the nutrient limitation term is visable as a strong inter-annual coherence between diatoms and phosphate as well as NUTLIM before 1940. After 1940 NUTLIM ~~as well as~~ and the concentrations of the individual phytoplankton

15

species ~~has~~ have gained such high values that smaller inter-annual variations have little effect on the production. Similarily, the less nutrient sensitive group flagellates shows much smaller inter-annual coherence with phosphate even before 1940. NUTLIM for this group is already high enough so that small long-term variations do not reflect strongly in the results.

Very little inter-annual coherence is visable also between phytoplankton and nitrogen. The spring bloom is phosphate limited throughout the run except for a few years after 1990 where diatoms display nitrogen limitation. The much weaker diatom and flagellate autumn bloom displays no inter-annual coherence with DIN most likely due to the high NUTLIM levels.

The shift in nutrient limitation patterns is also visable in a slight forward shift in the month of maximum mixed layer NUTLIM for diatoms after 1980, although a similar shift cannot be seen for flagellates. Below the mixed layer, maximum NUTLIM shifts significantly towards late summer for both diatoms and flagellates. Furthermore, the annual maximum of total chlorophyll concentration (Diatoms + Flagellates + Cyanobacteria) displayed a few years at the end of the run where the maximum corresponded to the autumn bloom due to the large increase in cyanobacteria. This is in agreement with Kahru et al. (2016) who found from satellite data that the annual chlorophyll maximum has shifted from the spring bloom maximum in May to the cyanobacteria bloom in July.

Riverine input of nutrients is an extremely important variable in the Baltic Sea and the large increase during the 20th century has initiated spreading of anoxic bottoms (Carstensen et al., 2014) . We found quite strong coherence between riverine input of DIN and mixed layer DIN but not a similar relationship between riverine phosphate input and the corresponding mixed layer concentration. As mixed layer salinity displayed in-phase inter-annual coherence with phosphate and only weak anti-phase coherence with DIN we hypothesise that this is due to a greater importance of the flux of phosphate from lower layers.

The mixed layer temperature in the Baltic Proper has increased during the 20th century. We found some response of this mainly from the most temperature sensitive phytoplankton group cyanobacteria during periods of large interannual temperature increases. Flagellates, being more temperature sensitive than diatoms, seems to display a coherence with the temperature increase occuring after 1980.

Variations in mixed layer depth affects mainly diatoms as these have a high sinking ~~speed~~velocity. In-phase coherence on periodicities shorter than one year indicates that large seasonal changes in the mixed layer depth significantly affects the mixed layer concentrations while smaller interannual variations are of little consequence.

~~Finally, the effect of irradiance on primary production was scrutinized. However, interannual irradiance variations have very little effect on the primary production~~Irradiance displayed very little coherence with phytoplankton biomass.

In conclusion, ~~interannual variations have affected the primary production mostly through the limiting nutrient phosphate before 1950 in our model run.~~ through studying inter-annual wavelet coherence between simulated phytoplankton biomass and key variables we have found that phytoplankton showed strong coherence with the limiting nutrient before 1950. After that nutrients and phytoplankton exists in the water column at such high concentrations that smaller interannual variations have much less effect. Furthermore, the mixed layer concentrations of DIN show strong interannual coherence with riverine DIN input while riverine phosphate displays almost no coherence with the corresponding mixed layer concentration. Instead, in-phase coherence with mixed layer salinity indicates a stronger importance of mixing with lower layers. ~~Expanding low oxygen conditions in the deep water has resulted in a shift in the composition of nutrients. In the model, this results in seasonality in~~

493 ~~the nutrient limitation pattern of the mixed layer with phosphate limitation in the spring and nitrogen limitation after the spring~~

494 ~~bloom~~ Temperature displays some inter-annual coherence with the more temperature sensitive flagellates.

## 5   Data availability

496 The model data on which the results in the present study are based on are stored and available from the Swedish Meteorological

497 and Hydrological Institute. Please send your request to ocean.data@smhi.se.

# 509 References

510 Almroth-Rosell, E., Eilola, K., Meier, H. E. M., and Hall, P. O. J.: Transport of fresh and resuspended particulate organic material in the
511    Baltic Sea - a model study, Journal of Marine Systems, doi:doi:10.1016/j.jmarsys.2011.02.005, 2011.

512 Carey, C. C., Hanson, P. C., Lathrop, R. C., and St. Amand, A. L.: Using wavelet analyses to examine variability in phytoplankton seasonal
513    succession and annual periodicity, Journal of Plankton Research, 38, 27–40, doi:10.1093/plankt/fbv116, http://www.plankt.oxfordjournals.
514    org/lookup/doi/10.1093/plankt/fbv116, 2016.

515 Carstensen, J., Andersen, J. H., Gustafsson, B. G., and Conley, D. J.: Deoxygenation of the Baltic Sea during the last century, Proceed-
516    ings of the National Academy of Sciences, 111, 5628–5633, doi:10.1073/pnas.1323156111, http://www.pnas.org/cgi/doi/10.1073/pnas.
517    1323156111, 2014.

518 Cazelles, B., Chavez, M., Berteaux, D., Ménard, F., Vik, J. O., Jenouvrier, S., and Stenseth, N. C.: Wavelet analysis of ecological time series,
519    Oecologia, 156, 287–304, doi:10.1007/s00442-008-0993-2, 2008.

520 Conley, D. J., Humborg, C., Rahm, L., Savchuk, O. P., and Wulff, F.: Hypoxia in the Baltic Sea and Basin-Scale Changes in Phosphorus
521    Biogeochemistry, Environ. Sci. Technol., 36, 5315–5320, doi:10.1021/es025763w, 2002.

522 Conley, D. J., Björck, S., Bonsdorff, E., Carstensen, J., Destouni, G., Gustafsson, B. G., Hietanen, S., Kortekaas, M., Kuosa, H., Markus
523    Meier, H. E., Müller-Karulis, B., Nordberg, K., Norkko, A., Nürnberg, G., Pitkänen, H., Rabalais, N. N., Rosenberg, R., Savchuk, O. P.,
524    Slomp, C. P., Voss, M., Wulff, F., and Zillén, L.: Hypoxia-Related Processes in the Baltic Sea, Environmental Science & Technology, 43,
525    3412–3420, doi:10.1021/es802762a, http://pubs.acs.org/doi/abs/10.1021/es802762a, 2009.

526 Dortch, Q.: The interaction between ammonium and nitrate uptake in phytoplankton, Marine Ecology Progress Series, 61, 183–201,
527    doi:10.3354/meps061183, 1990.

528 Droop, M.: Some thoughts on nutrient limitation in algae, Journal of Phycology, 9, 264–272, doi:10.1111/j.1529-8817.1973.tb04092.x, 1973.

529 Eilola, K., Meier, H. E. M., and Almroth, E.: On the dynamics of oxygen, phosphorus and cyanobacteria in the Baltic Sea; A model study,
530    Journal of Marine Systems, 75, 163–184, doi:10.1016/j.jmarsys.2008.08.009, http://dx.doi.org/10.1016/j.jmarsys.2008.08.009, 2009.

531 Eilola, K., Gustafsson, B. G., Kuznetsov, I., Meier, H. E. M., Neumann, T., and Savchuk, O. P.: Evaluation of biogeochemical
532    cycles in an ensemble of three state-of-the-art numerical models of the Baltic Sea, Journal of Marine Systems, 88, 267–284,
533    doi:10.1016/j.jmarsys.2011.05.004, http://dx.doi.org/10.1016/j.jmarsys.2011.05.004, 2011.

534 Eilola, K., Mårtensson, S., and Meier, H. E. M.: Modeling the impact of reduced sea ice cover in future climate on the Baltic Sea biogeo-
535    chemistry, Geophysical Research Letters, 40, 149–154, doi:10.1029/2012GL054375, 2013.

536 Eilola, K., Almroth-Rosell, E., and Meier, H. E. M.: Impact of saltwater inflows on phosphorus cycling and eutrophication in the Baltic Sea:
537    a 3D model study, Tellus A, http://dx.doi.org/10.3402/tellusa.v66.23985, 2014.

538 Flynn, K. J.: Ecological modelling in a sea of variable stoichiometry: Dysfunctionality and the legacy of Redfield and Monod, Progress in
539    Oceanography, 84, 52–65, doi:10.1016/j.pocean.2009.09.006, http://dx.doi.org/10.1016/j.pocean.2009.09.006, 2010.

540 Graham, L. P.: Modeling runoff to the Baltic Sea, Ambio, 28, 328–334, 1999.

541 Granéli, E., Wallström, K., Larsson, U., Granéli, W., and Elmgren, R.: Nutrient limitation of primary production in the Baltic Sea Area,
542    Ambio, 19, 1990.

543 Grinsted, a., Moore, J. C., and Jevrejeva, S.: Application of the cross wavelet transform and wavelet coherence to geophysical time series,
544    Nonlinear Processes in Geophysics, 11, 561–566, doi:10.5194/npg-11-561-2004, http://www.nonlin-processes-geophys.net/11/561/2004/,
545    2004.

546     Gustafsson, B. G., Schenk, F., Blenckner, T., Eilola, K., Meier, H. E. M., Müller-Karulis, B., Neumann, T., Ruoho-Airola, T., Savchuk, O. P.,

547        and Zorita, E.: Reconstructing the development of baltic sea eutrophication 1850-2006, Ambio, 41, 534–548, doi:10.1007/s13280-012-

548        0318-x, 2012.

549     Hansson, D., Eriksson, C., Omstedt, A., and Chen, D.: Reconstruction of river runoff to the Baltic Sea, AD 1500-1995, International Journal

550        of Climatology, 31, 696–703, doi:10.1002/joc.2097, 2011.

551     HELCOM: Approaches and methods for eutrophication target setting in the Baltic Sea region., Balt. Sea Env. Proc. No. 1, 2012., 2012.

552     Jackett, D. R., McDougall, T. J., Feistel, R., Wright, D. G., and Griffies, S. M.: Algorithms for density, potential temperature, con-

553        servative temperature, and the freezing temperature of seawater, Journal of Atmospheric and Oceanic Technology, 23, 1709–1728,

554        doi:10.1175/JTECH1946.1, 2006.

555     Jakobsen, H. H. and Markager, S.: Carbon-to-chlorophyll ratio for phytoplankton in temperate coastal waters: Seasonal patterns and rela-

556        tionship to nutrients, Limnol. Oceanogr., 61, 1853–1868, doi:10.1002/lno.10338, 2016.

557     Kahru, M., Elmgren, R., and Savchuk, O. P.: Changing seasonality of the Baltic Sea, Biogeosciences, 13, 1009–1018, doi:10.5194/bg-13-

558        1009-2016, 2016.

559     Lau, K. and Weng, H.: Climate signal detection using wavelet transform: How to make a time series sing, Bulletin of the American Meteo-

560        rological Society, 76, 2391–2402, doi:10.1175/1520-0477(1995)076<2391:csduwt>2.0.co;2, 1995.

561     Meier, H. E. M. and Kauker, F.: Modeling decadal variability of the Baltic Sea : 2 . Role of freshwater inflow and large-scale atmospheric

562        circulation for salinity, Journal of Geofphysical Research, 108, 1–16, doi:10.1029/2003JC001799, 2003.

563     Meier, H. E. M., Döscher, R., and Faxén, T.: A multiprocessor coupled ice- ocean model for the Baltic Sea: application to the salt inflow.,

564        Journal of geophysical research, 108, doi:10.1029/2000JC000521, 2003.

565     Meier, H. E. M., Andersson, H. C., Arheimer, B., Blenckner, T., Chubarenko, B., Donnelly, C., Eilola, K., Gustafsson, B. G., Hansson, A.,

566        Havenhand, J., Höglund, A., Kuznetsov, I., MacKenzie, B. R., Müller-Karulis, B., Neumann, T., Niiranen, S., Piwowarczyk, J., Raudsepp,

567        U., Reckermann, M., Ruoho-Airola, T., Savchuk, O. P., Schenk, F., Schimanke, S., Väli, G., Weslawski, J.-M., and Zorita, E.: Comparing

568        reconstructed past variations and future projections of the Baltic Sea ecosystem—first results from multi-model ensemble simulations,

569        Environmental Research Letters, 7, 034 005, doi:10.1088/1748-9326/7/3/034005, 2012.

570     Meier, H. E. M., Höglund, A., Eilola, K., and Almroth-Rosell, E.: Impact of accelerated future global mean sea level rise on hypoxia in the

571        Baltic Sea, Climate Dynamics, pp. 1–10, doi:10.1007/s00382-016-3333-y, 2016.

572     Parker, R. A.: Dynamic models for ammonium inhibition of nitrate uptake by phytoplankton, Ecological Modelling, 66, 113–120,

573        doi:10.1016/0304-3800(93)90042-Q, 1993.

574     Redfield, A. C.: The biological control of chemical factors in the environment, American Scientist, 46, 205–221, doi:10.5194/bg-11-1599-

575        2014, 1958.

576     Ruoho-Airola, T., Eilola, K., Savchuk, O. P., Parviainen, M., and Tarvainen, V.: Atmospheric nutrient input to the baltic sea from 1850 to

577        2006: A reconstruction from modeling results and historical data, Ambio, 41, 549–557, doi:10.1007/s13280-012-0319-9, 2012.

578     Savchuk, O. P.: Large-Scale Dynamics of Hypoxia in the Baltic Sea, in: Chemical structure of pelagic redox interfaces: Observation and

579        modeling, Hdb Env Chem, edited by Yakushev, E. V., pp. 137–160, Springer-Verlag, Berlin Heidelberg, doi:10.1007/698_2010_53, 2010.

580     Savchuk, O. P., Wulff, F., Hille, S., Humborg, C., and Pollehne, F.: The Baltic Sea a century ago — a reconstruction from model simulations,

581        verified by observations, Journal of Marine Systems, 74, 485–494, doi:10.1016/j.jmarsys.2008.03.008, http://linkinghub.elsevier.com/

582        retrieve/pii/S0924796308000572, 2008.

583  Savchuk, O. P., Gustafsson, B. G., Rodríguez, M., Sokolov, A. V., and Wulff, F. V.: External nutrient loads to the Baltic Sea , 1970-2006,
584      2012.

585  Schernewski, G. and Neumann, T.: The trophic state of the Baltic Sea a century ago: a model simulation study, Journal of marine systems,
586      53, 109–124, doi:https://doi.org/10.1016/j.jmarsys.2004.03.007, 2004.

587  Schimanke, S. and Meier, H.: Decadal to centennial variability of salinity in the Baltic Sea, Journal of Climate, pp. JCLI–D–15–0443.1,
588      doi:10.1175/JCLI-D-15-0443.1, http://journals.ametsoc.org/doi/10.1175/JCLI-D-15-0443.1, 2016.

589  Siegel, H., Gerth, M., and Tschersich, G.: Sea surface temperature development of the Baltic Sea in the period, Oceanologia, 48, 119–131,
590      2006.

591  Tamminen, T. and Andersen, T.: Seasonal phytoplankton nutrient limitation patterns as revealed by bioassays over Baltic Sea gradients of
592      salinity and eutrophication, Marine Ecology Progress Series, 340, 121–138, doi:10.3354/meps340121, 2007.

593  Torrence, C. and Compo, G. P.: A practical guide to wavelet analysis, Bull. Amer. Meteor. Soc., pp. 61–78, 1998.

594  Tyrrell, T.: The relative influences of nitrogen and phosphorus on oceanic primary production, Nature, 400, 525–531, 1999.

595  Vahtera, E., Conley, D. J., Gustafsson, B. G., Kuosa, H., Pitkanen, H., Savchuk, O. P., Tamminen, T., Viitasalo, M., Wasmund, N., and Wulff,
596      F.: Internal Ecosystem Feedbacks Enhance Nitrogen-fixing Cyanobacteria., Ambio, 36, 186–193, 2007.

597  Winder, M. and Cloern, J. E.: The annual cycles of phytoplankton biomass., Philosophical transactions of the Royal Society of London.
598      Series B, Biological sciences, 365, 3215–26, doi:10.1098/rstb.2010.0125, http://rstb.royalsocietypublishing.org/content/365/1555/3215,
599      2010.
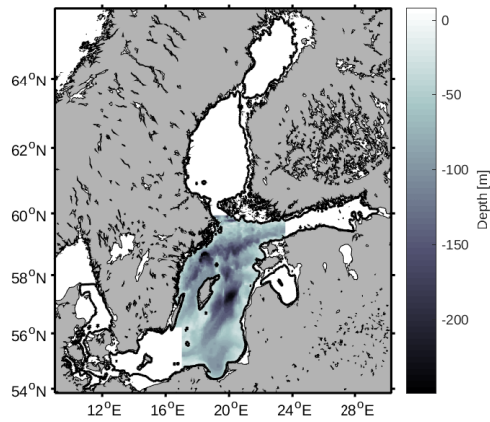
**Figure 1.** Study area. The grey scale represents depth in m.
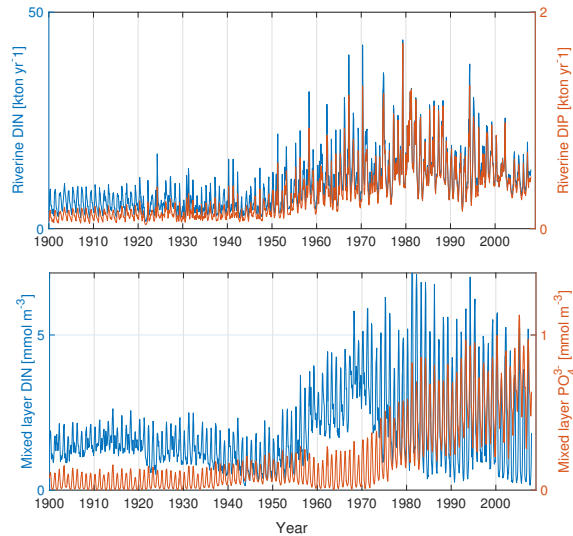


**Figure 2.** The top panel shows riverine ~~phosphate loads~~ DIN (blue) and ~~mixed layer concentration of~~ phosphate (red) ~~and the~~ loads. The bottom panel shows ~~riverine~~ mixed layer DIN (blue) and ~~mixed layer DIN~~ phosphate (red).

600 ~~Modelled basin integrated chlorophyll compared to observations. (a) shows observations (blue) and model results (red) for~~
601 ~~the period 1990-2009 together with model results for the period 1880-1999 (yellow). The lower three panels shows the wavelet~~
602 ~~spectra for (b) observations, (c) model results for 1990-2009 and (d) model results for the period 1880-1899. The y-axis shows~~
603 ~~the periodicity and the colors represent the wavelet power. The black curves in the wavelet figures represent the 95% confidence~~
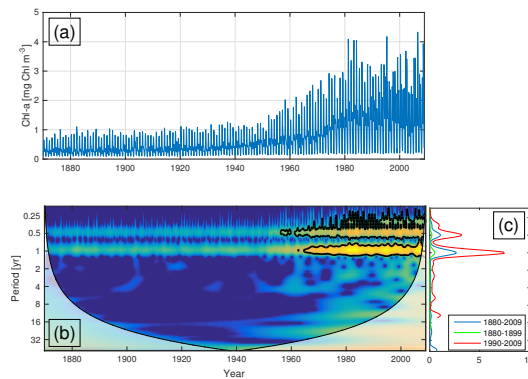
**Figure 3.** ~~Wavelet coherence between riverine phosphate and mixed layer phosphate concentration~~ Time-series of phytoplankton biomass (~~top~~a) together with the corresponding wavelet power spectrum (b) and ~~riverine DIN and surface DIN concentration~~ global wavelet spectrum (~~bottom~~c). More yellow means more power. The ~~arrows indicates~~ black curves in (b) represent the ~~phase lag. When pointing~~ 95% confidence level relative to red noise. The white areas in (b) represent the ~~right~~ cone of influence in which the ~~two time-series~~ results are ~~in phase~~ impacted by edge-effects and ~~when pointing in the opposite direction anti-phase~~are therefore not shown. The ~~right panels show~~ different lines in represent the ~~integrated coherence for the whole period~~ global spectrum 1880-2009 (blue)~~and before~~, 1880-1899 (green)~~and after~~, 1990-2009 (red)~~1950.~~.

604 ~~level relative to an AR1 spectrum. (e), (f) and (g) show the corresponding global power spectra together with the AR1 spectrum~~
605 ~~(red). The white areas in the wavelet figures represents the cone of influence in which the results are impacted by edge-effects~~
606 ~~and are therefore not shown.~~
607 ~~Time-series of anoxic volume (top), below mixed layer concentrations of phosphate (blue) and DIN (nitrate + ammonium,~~
608 ~~red) (middle) and nitrate (blue) and ammonium (red)(bottom).~~
609 ~~Time-series of mixed layer phosphate (blue) and DIN (nitrate + ammonium, red) concentration (middle) and nitrate (blue)~~
610 ~~and ammonium (red) concentration (bottom).~~
611 ~~Wavelet coherence between mixed layer NUTLIM and diatoms (top), flagellates (middle) and cyanobacteria (bottom).~~
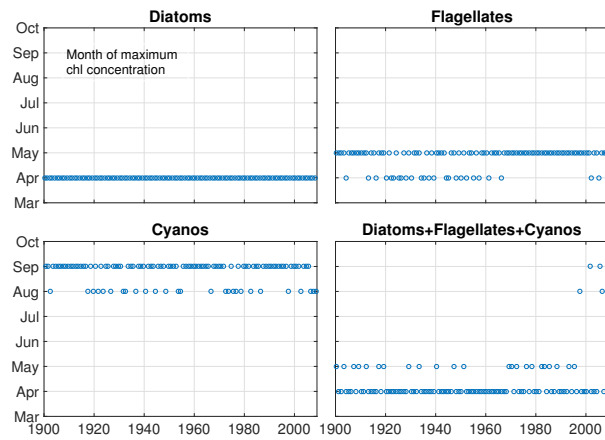
**Figure 4.** ~~Wavelet coherence between mixed layer salinity and phosphate~~ The month of maximum concentration ~~(top)~~ of diatoms, flagellates and ~~mixed layer salinity and nitrate concentration (bottom)~~cyanobacteria as well as their sum.~~The right panels show the integrated coherence spectrum.~~
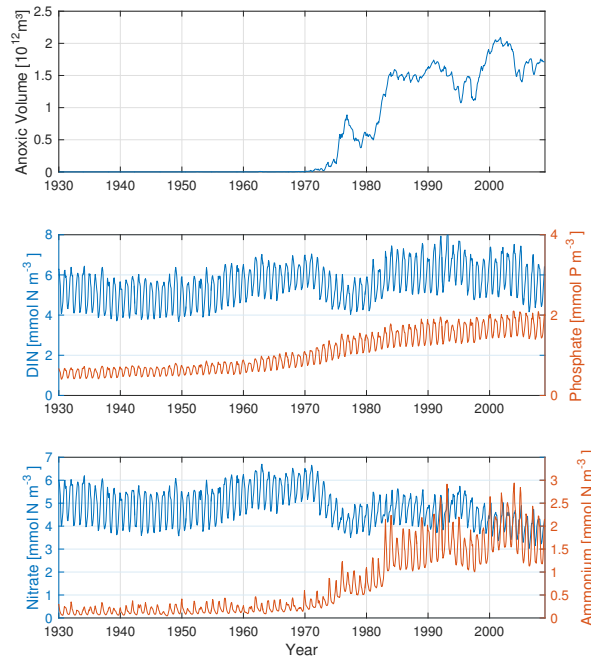
**Figure 5.** ~~Wavelet coherence between riverine phosphate and diatoms~~ Time-series of anoxic volume (top), ~~flagellates~~ below mixed layer concentrations of DIN (nitrate + ammonium, blue) and phosphate (red) (middle) and ~~cyanobacteria~~ nitrate (blue) and ammonium (red)(bottom).~~The right panels show the integrated spectrum.~~

24
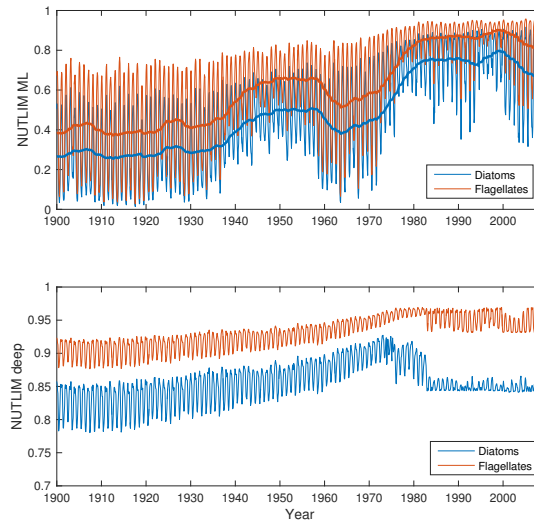
**Figure 6.** ~~Wavelet coherence between riverine DIN and diatoms~~ Time-series of nutrient limitation in the mixed layer (top) ~~, flagellates~~ and below (~~middle~~bottom) for diatoms (blue) and ~~cyanobacteria~~ flagellates (~~bottom~~red). The ~~right panels~~ thicker lines in the top panel show the ~~integrated spectrum~~5yr moving average.
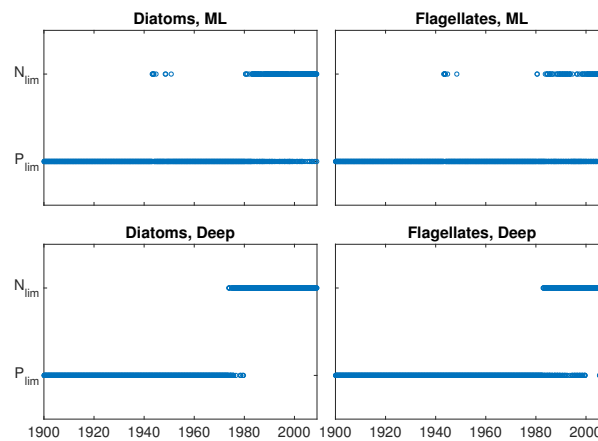


**Figure 7.** Nitrogen or phosphate limitation as function of time in the mixed layer (upper panels) and in the deep water (lower panels) of diatoms (left panels) and flagellates (right panels). Note that simultaneous N and P limitation is not possible although the size of the rings in the figures gives this appearence.
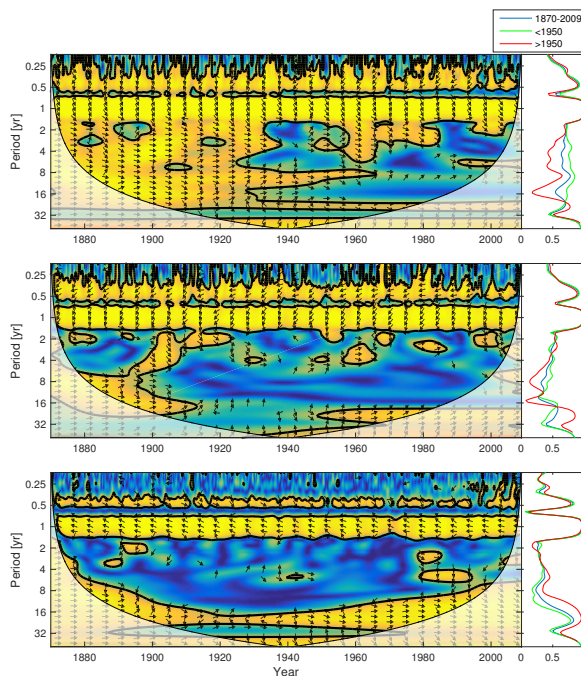
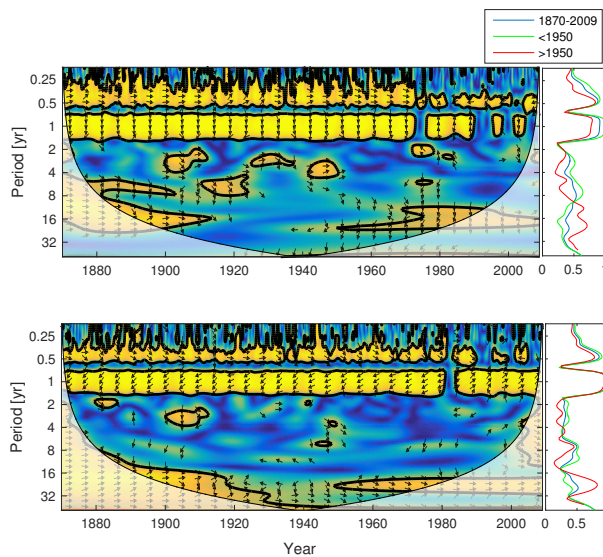**Figure 8.** Wavelet coherence between mixed layer phosphate concentration and diatoms (top), flagellates (middle) and cyanobacteria (bottom). More yellow means more coherence. The arrows indicate the phase lag. When pointing to the right the two time-series are in phase and when pointing in the opposite direction anti-phase. The right panels show the coherence averaged over the whole period (blue) and before (green) and after (red) 1950.
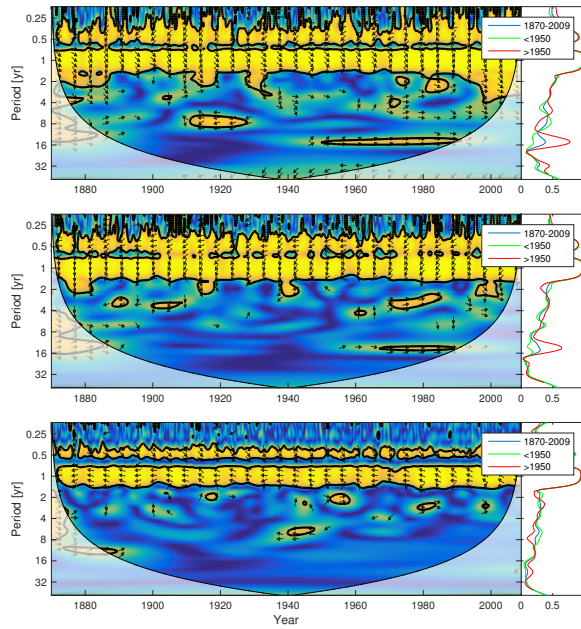
**Figure 9.** Wavelet coherence between mixed layer DIN concentration and diatoms (top), flagellates (middle) and cyanobacteria (bottom).



**Figure 10.** Wavelet coherence between deep water NUTLIM and diatoms (top), flagellates (middle)and cyanobacteria (bottom)

27
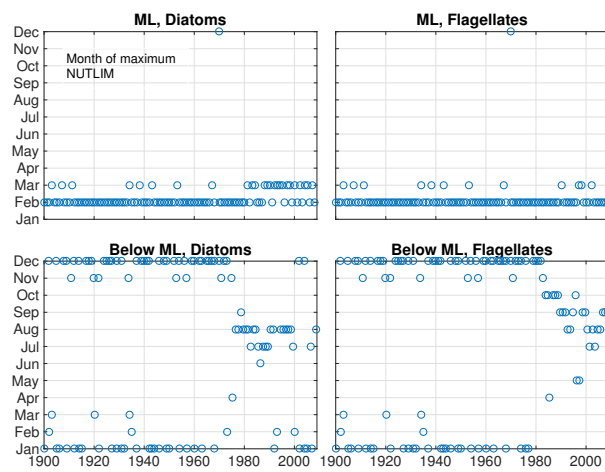
**Figure 11.** The month of maximum NUTLIM for diatoms (left) and flagellates (right) in the mixed layer (top) and below (bottom).
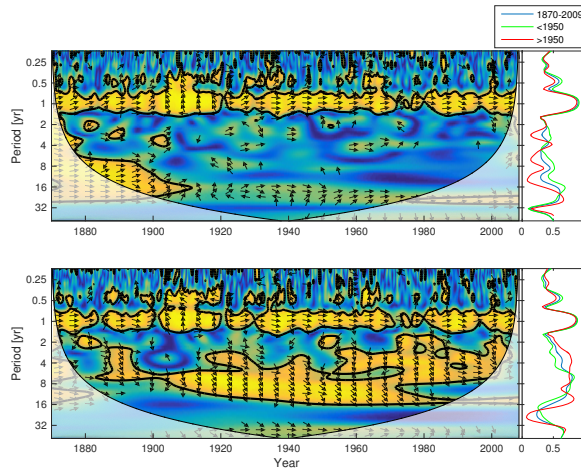
**Figure 12.** ~~The month of maximum~~ Wavelet coherence between riverine phosphate and mixed layer phosphate concentration ~~of diatoms, flagellates~~ (top) and ~~cyanobacteria as well as their sum~~ riverine DIN and mixed layer DIN concentration (bottom). The arrows indicates the phase lag. When pointing to the right the two time-series are in phase and when pointing in the opposite direction anti-phase. The right panels show the averaged coherence for the whole period (blue) and before (green) and after (red) 1950.
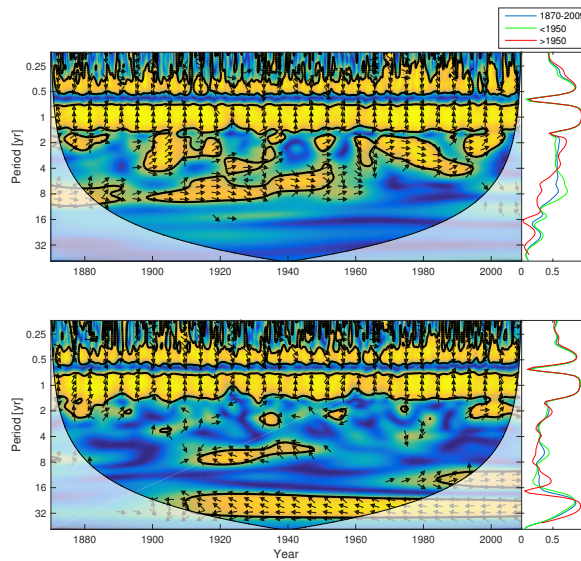


**Figure 13.** Wavelet coherence between mixed layer salinity and phosphate concentration (top) and mixed layer salinity and nitrate concentration (bottom). The right panels show the averaged coherence spectrum.
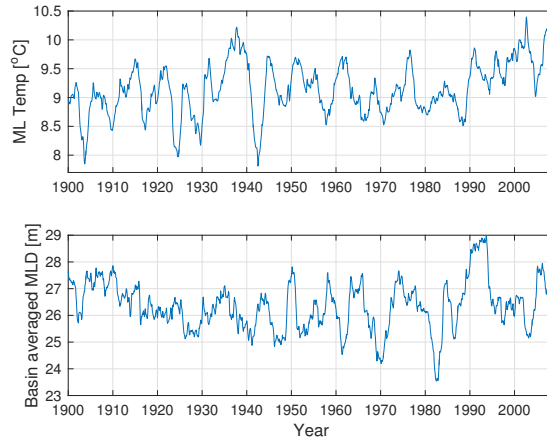
29

**Figure 14.** 2-yr moving average of mixed layer temperature (top) and mixed layer depth (bottom).
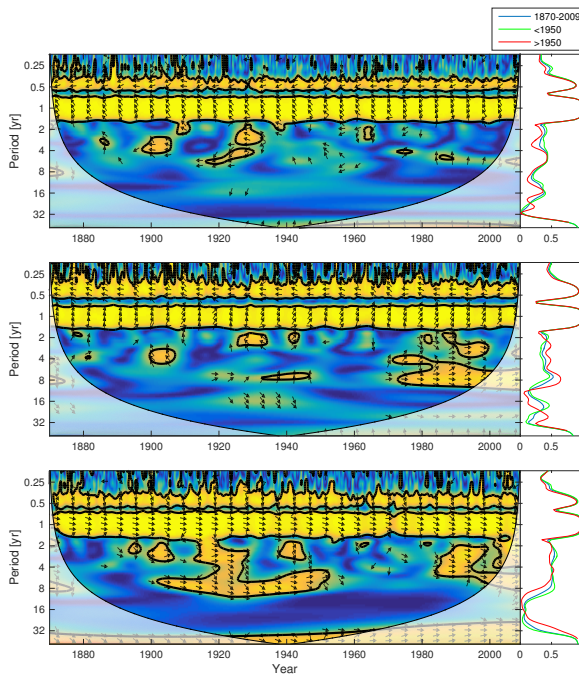


**Figure 15.** Wavelet coherence between mixed layer temperature and diatoms (top), flagellates (middle) and cyanobacteria (bottom).
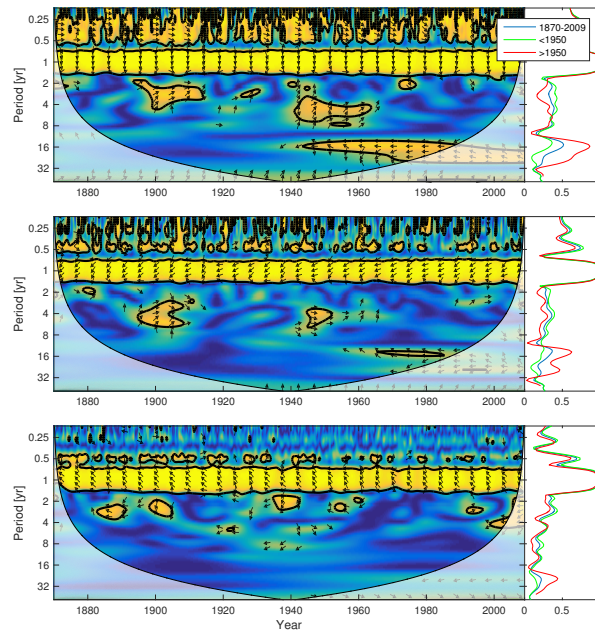
**Figure 16.** Wavelet coherence between mixed layer depth and diatoms (top), flagellates (middle) and cyanobacteria (bottom).